ACS OMEGA

Open Access

http://pubs.acs.org/journal/acsodf

Article

Improving the Interfacial Adhesion of Long Carbon Fiber-Reinforced Polyamide 6 Composites by Electrochemical Oxidation and Polyethylenimine-Carboxymethyl Cellulose Grafting

Emine C. Gokce, Melike Gungor, Ali Kilic,* and Mahmut Ercan Acma

Cite This: *ACS Omega* 2024, 9, 32547−32556

Read Online

ACCESS | Metrics & More | Article Recommendations

ABSTRACT: Carbon fiber (CF)-reinforced thermoplastic composites have notable ascents in various sectors and applications. For high-performance composites, strong interfacial adhesion between the polymer matrix and the CF is crucial. This is achieved by introducing functional groups on the CF surface. In this paper, a water-based surface treatment was applied to long carbon fibers to enhance the interfacial bonding with the polyamide 6 (PA6) matrix. For that, PEI and CMC were grafted onto the surface of carbon fibers after electrochemical oxidation. The PEI-CMC sizing reduced the carbon fiber/water contact angle to 26.42° from 111.69°. The clear improvement in wettability resulted in a 164.8% increase in the interfacial strength of 26.7 MPa after the application of PEI-CMC sizing on carbon fibers (CFs). The resultant tensile and flexural strength increased by 19.3 and 11.7% from 2009.6 and 378.3 MPa for desized CF/PA6 composites to 250.3 and 422.7 MPa for PEI-CMC-sized CF/PA6 composites, respectively. Moreover, the fractured surface morphologies were also investigated to confirm the enhancement of mechanical properties. The proposed one-step electrochemical oxidation and water-based sizing procedure is found to be promising for the production of high-performance long-fiber-reinforced thermoplastic composites.

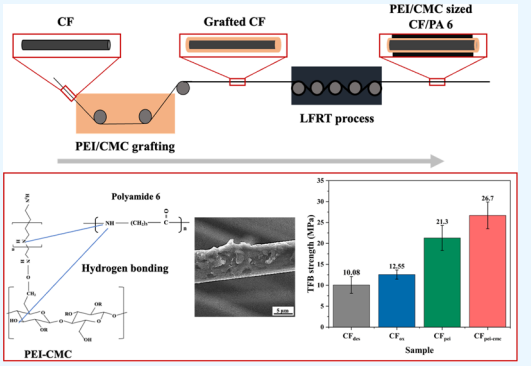

1. INTRODUCTION

Since the mid-1960s, carbon fiber-reinforced polymers (CFRPs) have been widely used in various sectors, including automotive, aviation, construction, renewable energy, oil and gas, and sports equipment, due to their excellent mechanical, thermal, and electrical properties.[1] On the other hand, the carbon fiber (CF)-reinforced thermoplastic composites have gained crucial importance for the rising concerns on recyclability and sustainability.[2,3] PA6 is widely used for its remarkable impact resistance and repeated recyclability. However, achieving homogeneous impregnation onto each CF surface is still challenging due to its high melt viscosity.[4] It is widely acknowledged that the mechanical performance of composites is predominantly influenced by the load transfer from the matrix to the fibers.[5] Moreover, the low interfacial bonding between the virgin CFs and the polymer matrix, due to the smooth, hydrophobic, and chemically inert nature of CFs,[6,7] has long been a serious issue that needs to be overcome.

In the past few years, a great deal of attempts have made to enhance the mechanical performance of composites using surface treatment methods such as plasma treatment,[8,9] electrochemical oxidation,[10,11] acidic oxidation,[12,13] sizing,[14,15] and grafting.[16,17] Although plasma treatment and oxidation methods can increase the interfacial bonding between the CF and the matrix by formation of functional groups (−OH and −COOH) on the CF surface, intentional oxidation can cause a serious reduction in the CF strength.[18,19] To minimize the impact on the mechanical properties of CFs during oxidation, different sizing materials like silane coupling agents can be grafted onto CF surfaces.[20]

On the other hand, water-based sizing (grafting) agents have the potential to reduce environmental pollution in surface treatment processes. Among them, due to its nontoxicity and low costs, CMC has long been used as the sizing material for fibers.[21] Given that the glucopyranose ring of CMC possesses numerous hydroxyl groups, it can further enhance the wetting properties of the CF surface.[22] Qiu et al. reported the effect of CMC sizing on carbon fiber surface defects for epoxy matrix composites.[23] The CF surface was coated with solutions containing different concentrations of CMC, and they observed that the contact angle decreased from 120.4 to 85.9°. They discovered that the interlaminar shear strength

Received: February 8, 2024
Revised: June 7, 2024
Accepted: July 4, 2024
Published: July 18, 2024

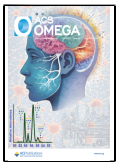

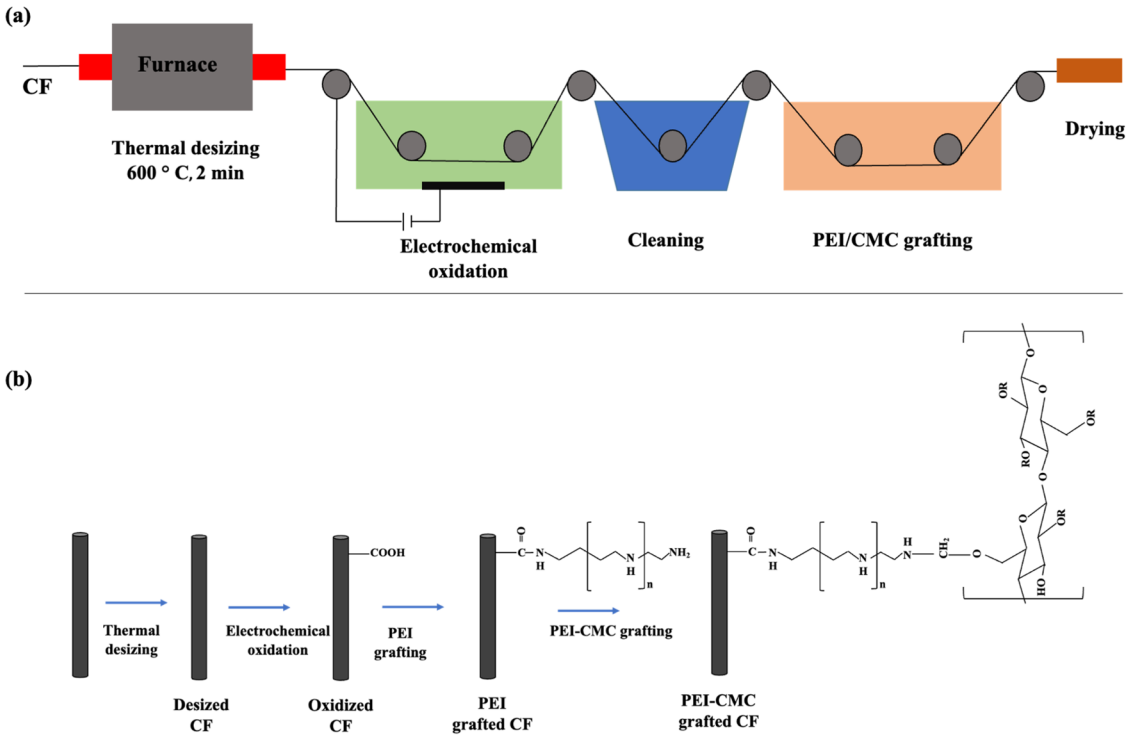

Figure 1. Schematic illustration of the surface treatment of CFs (a) and chemical reactions occurring on the CF surface (b).

(ILSS) of the CF treated with 0.075 g CMC is 18.09% higher than that of virgin CFs. In another study, graphene oxide (GO)/CMC sizing was applied to enhance the interfacial adhesion between the CF and the epoxy.[24] It was observed that the contact angle value decreased to 82.6° after surface treatment using GO/CMC, while the ILSS value increased by 58.60% compared to untreated CFs. These studies have demonstrated that CMC leads to an increase in the interface adhesion between epoxy and the carbon fiber.

On the other hand, there are also studies related to cellulose-based reinforced PA6 composites. Peng et al. prepared cellulose [microcrystalline cellulose (MCC), cellulose nanofibrils (CNFs), and cellulose nanocrystals (CNC)]-reinforced PA6 composites by melt compounding and injection molding at 270 °C. The composite containing 10% MCC exhibited the highest tensile strength value of 63.5 MPa, representing a 13.5% increase compared to the control sample (PA6).[25] Kiziltas et al. conducted a study on the development of cellulosic fiber-reinforced PA6 composites via a Brabender Prep Mixer at 250 °C. The composite including 20 wt % reinforcement achieved the highest storage modulus (E') of 3960 MPa, which was 68% higher than that of control PA6.[26] Rahimi et al. investigated the dynamic mechanical properties of the CNC/PA6 composite which was produced by the anionic ring-opening polymerization followed by compression molding at 235 °C. The storage modulus of the composite with 2% CNC reached 2600 MPa from 1900 MPa compared to neat PA6.[27]

In this study, an effective method was proposed to enhance the interfacial adhesion between carbon fibers and the PA6 matrix. After electrochemical oxidation, the CF bundle was immersed in a CMC-modified polyethylenimine (PEI) solution. PEI-CMC formed a dense structure on the surface of CFs through a grafting reaction, introducing abundant active functional groups causing the formation of hydrogen bonding, thereby improving the wetting of CFs with PA6. The morphological and resultant mechanical properties of long-CF-reinforced PA6 composites were investigated. The proposed simple and environmentally friendly method is thought to be an alternative route for enhancing the interfacial characteristics of carbon fiber-reinforced composites.

2. MATERIALS AND METHODS

2.1. Materials. CF bundles (6K, d_{fiber} = 7 μm) with an epoxy sizing agent were purchased from DowAksa Company, Yalova, Türkiye. Ammonium bicarbonate (NH_4CO_3, 99%) was provided by bluechemia (Istanbul, Türkiye). Carboxymethyl cellulose (CMC, 800−1300 mPa·s) was donated by USK Kimya Inc. (Aydin, Türkiye). Polyethylenimine (PEI, average MW ∼ 25,000) was purchased from Sigma-Aldrich. Formaldehyde was obtained from bluechemia and used as is. PA6 chips were supplied by POLITEM Dynamic Plastic Co. Inc. (Tekirdag, Türkiye).

2.2. Preparation CMC-PEI Coating. In order to bind over the CF surface, CMC was initially grafted with PEI. CMC (0.5 g L^{-1}), PEI (5 g L^{-1}), and formaldehyde (0.5 g L^{-1}) were dissolved in deionized water. After that, the prepared solution was stirred for 1 h for the cross-linking of CMC and PEI to occur,.[28−30]

2.3. Surface Treatment. As shown in Figure 1a, prior to surface treatment, the carbon fiber bundles were desized at 600 °C for 2 min in an air atmosphere (called CF_{des}). In the second stage, electrochemical oxidation of CF_{des} was performed via a custom-made laboratory setup at room temperature (25 °C) to create functional groups on the surface and facilitate cross-linking with PEI-CMC. 7 wt % aqueous NH_4HCO_3 solution was used as the electrolyte. CF_{des} was chosen as the anode, while the graphite plate was used as the cathode. The treatment time was 80 s, while the distance between the anode and the cathode was kept at 3 cm, and the current density was

https://doi.org/10.1021/acsomega.4c01284
ACS Omega 2024, 9, 32547−32556

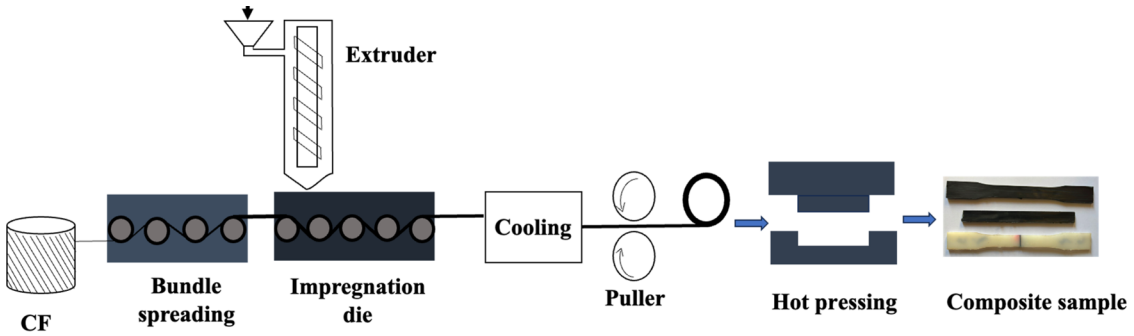

Figure 2. Whole fabrication process for unidirectional CF/PA6 samples.

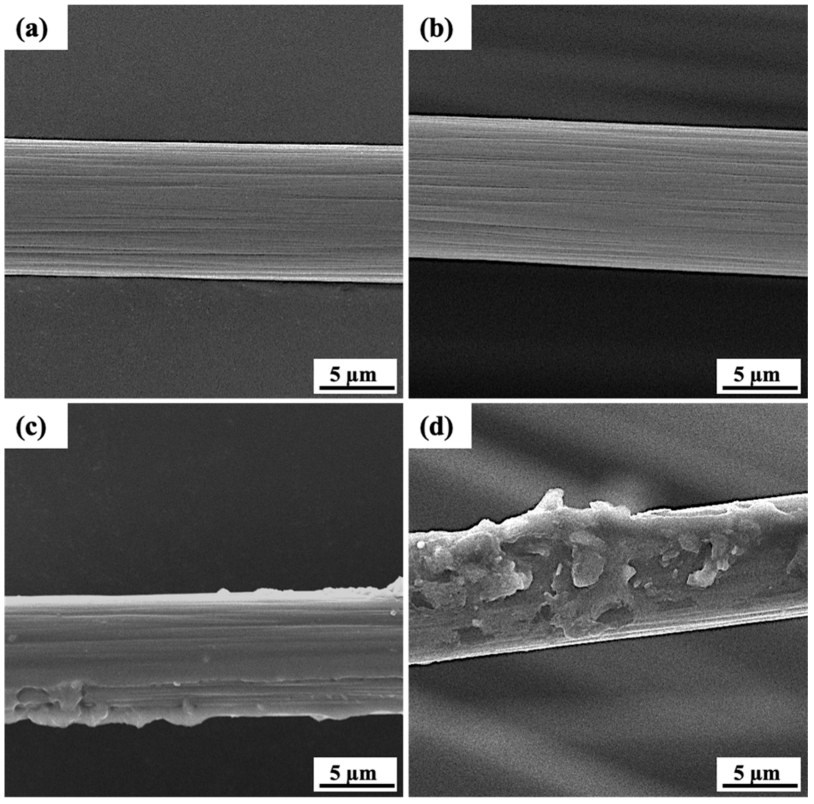

Figure 3. Morphologies of different CFs: desized CF (a), oxidized CF (b), PEI-sized CF (c), and PEI-CMC-sized CF (d).

set at 2 A m^{-2}. After oxidation, CFs were cleaned with deionized water followed by drying at 80 °C. The oxidized CF_{des} was named CF_{ox}.

Subsequently, CF_{ox} was passed through 5 wt % aqueous PEI solution. The PEI-coated CF_{ox} was denoted as CF_{pei}. On the other hand, CF_{ox} was submerged in the prepared PEI-CMC solution and called $CF_{pei-cmc}$. All chemical reactions occurring on the CF surface are illustrated in Figure 1b.

2.4. Preparation of Impregnated Sized CFs. The long-CF-reinforced PA6 prepregs were produced via melt impregnation employing an Areka Lab Scale LFRT line (Türkiye), which is composed of an impregnation apparatus, bundle spreading, an impregnation die (connected to an Areka E23D mini extruder), and cooling and pulling units, as illustrated in Figure 2. The prepared CF bundles were passed through the impregnation die where the molten PA6 resin was pumped continuously at 250 °C. The temperature profile of the extruder was 200, 220, and 240 °C.

The impregnated long-fiber bundles were then placed into dogbone-shaped and rectangular-shaped mechanical test dies. Composite samples were fabricated by hot pressing at 240 °C at a pressure of 7.5 MPa for 5 min.

2.5. Preparation of Transverse Fiber Bundle Samples. Dogbone-shaped PA6 samples were initially prepared via a hot press. Subsequently, a well-impregnated CF bundle was positioned in the center of the PA6 sample within a laboratory prepared mold. The mold was heated to 240 °C to facilitate the integration of the prepreg and PA 6 and then pressed at 5 MPa pressure for 5 min.

3. CHARACTERIZATION

3.1. Morphologies of Samples. The surface morphologies of virgin and functionalized carbon fibers were observed using a scanning electron microscope (TESCAN VEGA3). The fractured morphologies of composites were also analyzed by scanning electron microscopy (SEM). Images were captured at different magnifications ranging from 1000× and

https://doi.org/10.1021/acsomega.4c01284
ACS Omega 2024, 9, 32547−32556

10,000×. Prior to SEM, the samples were coated with gold−palladium (AuPd) to form a thin conductive layer.

3.2. Contact Angle Measurements. The wettability characteristics of CF bundles were evaluated by a Theta Lite contact angle meter (Terralab, Türkiye). 6 μL of deionized water (γ^d = 21.8 mN m $^{-1}$; γ = 72.8 mN m^{-1}) was used as the test liquid at room temperature (RT, 25 ± 0.5 °C).

3.3. Fourier Transform Infrared Spectroscopy of Sized CFs. The functional groups formed on the CF surface was analyzed via Fourier transform infrared (FTIR) spectroscopy (Nicolet iS150 spectrophotometer) from 500 to 4000 cm^{-1} with KBr pellet technique. The samples were characterized with a resolution of 4 cm^{-1}. All measurements were performed in a dry atmosphere at room temperature (RT, 25 ± 0.5 °C).

3.4. X-ray Photoelectron Spectroscopy. The chemical composition of the modified CF surface was investigated by X-ray photoelectron spectroscopy (XPS, ThermoFisher Scientific K-Alpha (Austria)) equipped with a monochromatic Al−Kα X-ray source (1486.6 eV). The binding energy of high-resolution C 1s spectra was adjusted to 284.5 eV as a reference.

3.5. Assessment of Interfacial Strength between CFs and PA6. In order to determine the interfacial strength, transverse fiber bundle (TFB) pull-out tests were conducted with a universal tensile test device (Shimadzu AG-IC series). The test device was set to a cross-head speed of 1 mm/min.

3.6. Mechanical Properties of CFs. The tensile test was applied using a Shimadzu testing machine AG-IC at a cross-head rate of 5 mm/min and a gauge length of 50 mm according to ASTM D638. Flexural testing was conducted in accordance with the procedure in ASTM D790 at a cross-head speed of 2 mm/min with a span length of 50 mm.

4. RESULTS AND DISCUSSION

4.1. Morphologies of Samples. Figure 3 shows SEM images of desized, oxidized, and PEI- and PEI-CMC-grafted carbon fibers denoted as CF_{des}, CF_{ox}, CF_{pei}, and $CF_{pei\text{-}cmc}$, respectively. As seen in Figure 3(a), the narrow grooves were formed on the surface of CF_{des} with longitudinal striations after thermal desizing. When the electrochemical oxidation was conducted, the surface of CF_{ox} did not clearly change, and it still had parallel grooves, as reported in the literature (Figure 3(b)).[31] In addition, as illustrated in Figure 3(c), PEI was successfully coated on the oxidized CF surface, and this can be seen in the formation of the thin layer on the CF_{pei} surface. Following PEI-CMC sizing, the topography of CFs changed considerably (Figure 3(d)). Therefore, several junction points were formed, which increased the mechanical interlocking, improving the interfacial bonding between CFs and PA6.

4.2. Contact Angle Measurements. The wettability of the CFs was determined via contact angle analysis, as given in Figure 4. As expected, the desized virgin CF (CF_{des}) exhibited high hydrophobicity (>110°). Thanks to considerable amounts of hydrophilic groups (OH and COOH) after electrochemical oxidation, the contact angle value of CF_{ox} decreased to 35.3° (Figure 4). Additionally, it was found that the contact angle values of CF_{pei} and $CF_{pei\text{-}cmc}$ decreased to 56.87 and 26.42°, respectively, due to the -NH- and −OH-based functionalities.

4.3. Fourier Transform Infrared Spectroscopy. Figure 5(a) shows the FTIR spectra of CF_{des}, CF_{ox}, CF_{pei}, and $CF_{pei\text{-}cmc}$. The peak at 3447 cm^{-1} corresponds to the stretching vibration of the −OH group because of the adsorbed water molecules on the CF surface. The peaks at about 2854−2925 cm^{-1} are assigned to the vibrations of C−H, and the peaks at 1635 and 1098 cm^{-1} are assigned to the stretching vibrations of C=C and C−C, respectively.[32] For CF_{ox}, the two new peaks emerged at 1168 and 1735 cm^{-1}, which are attributed to the C=O and C−O stretching vibrations of the carboxyl group after electrochemical oxidation, respectively. Due to oxidation, the OH peak intensity was decreased, and carboxyl peaks were observed.[33]

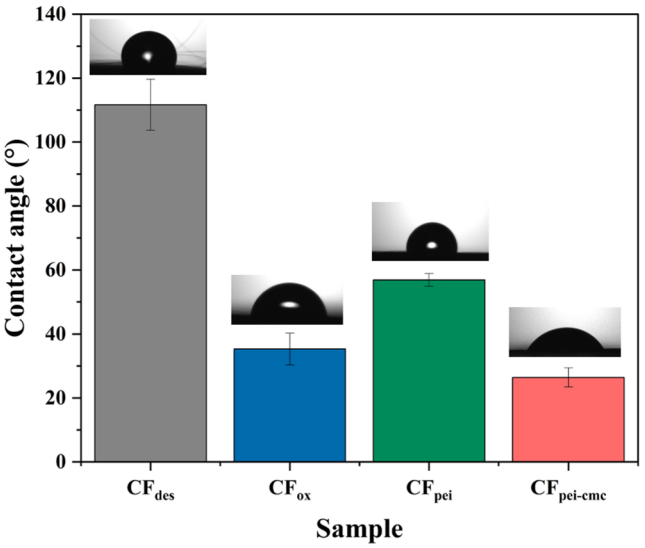

Figure 4. Contact angles of different carbon fibers.

Figure 5(b) shows the expected chemical reaction between PEI and CMC. Compared to CF_{ox}, there is an increase in the intensity of peak at 3447 cm^{-1} owing to N−H, which demonstrates the grafting reaction between CF_{ox} and PEI.[34] The transmittance peak near 1460 cm^{-1} is attributed to the C−N stretching vibrations from PEI.[35,36] As for the FTIR spectra of $CF_{pei\text{-}cmc}$, new peaks appeared at 1300−1700 cm^{-1}, which verifies the presence of PEI in the surface treatment materials. In addition, the peak around 1120 cm^{-1}, representing the C−N bond, also shows the successful grafting of PEI and CMC.[29] The increasing intensity of the C−O bond for the $CF_{pei\text{-}cmc}$ sample proves the presence of CMC. The peak in the range of 600−900 cm^{-1} is ascribed to the glucose structure of CMC.[23]

4.4. X-ray Photoelectron Spectroscopy. XPS analysis was employed to further examine the surface compositions of CF_{des}, CF_{ox}, CF_{pei}, and $CF_{pei\text{-}cmc}$. The survey spectra and calculated elemental percentages are displayed in Figure 6. The surface of CF_{ox} had a higher O/C ratio (0.29) than CF_{des} (0.03) because of the electrochemical oxidation of the desized CF. On the other hand, the N/C ratio on the surface of CF_{pei} (0.25) exceeded that of CF_{des} (0.02) due to the incorporation of PEI. This implies that the surfaces are rich in nitrogenous groups. In comparison to CF_{pei}, no dramatic change was observed in the N/C ratio for $CF_{pei\text{-}cmc}$. Nevertheless, its O/C ratio exhibited an increase (0.13) compared to that of CF_{pei} (0.08) due to the presence of carboxylic groups on the CMC. As for $CF_{pei\text{-}cmc}$, both the N/C ratio (0.25) and the O/C ratio (0.13) were notably elevated, indicating the efficient grafting of PEI-CMC onto the CF surfaces. This resulted in a substantial alteration of the elemental composition, enhancing the surface activity.

In order to further investigate the chemical states of the CF surface, the C 1s spectra were deconvoluted into curves with

https://doi.org/10.1021/acsomega.4c01284
ACS Omega 2024, 9, 32547−32556

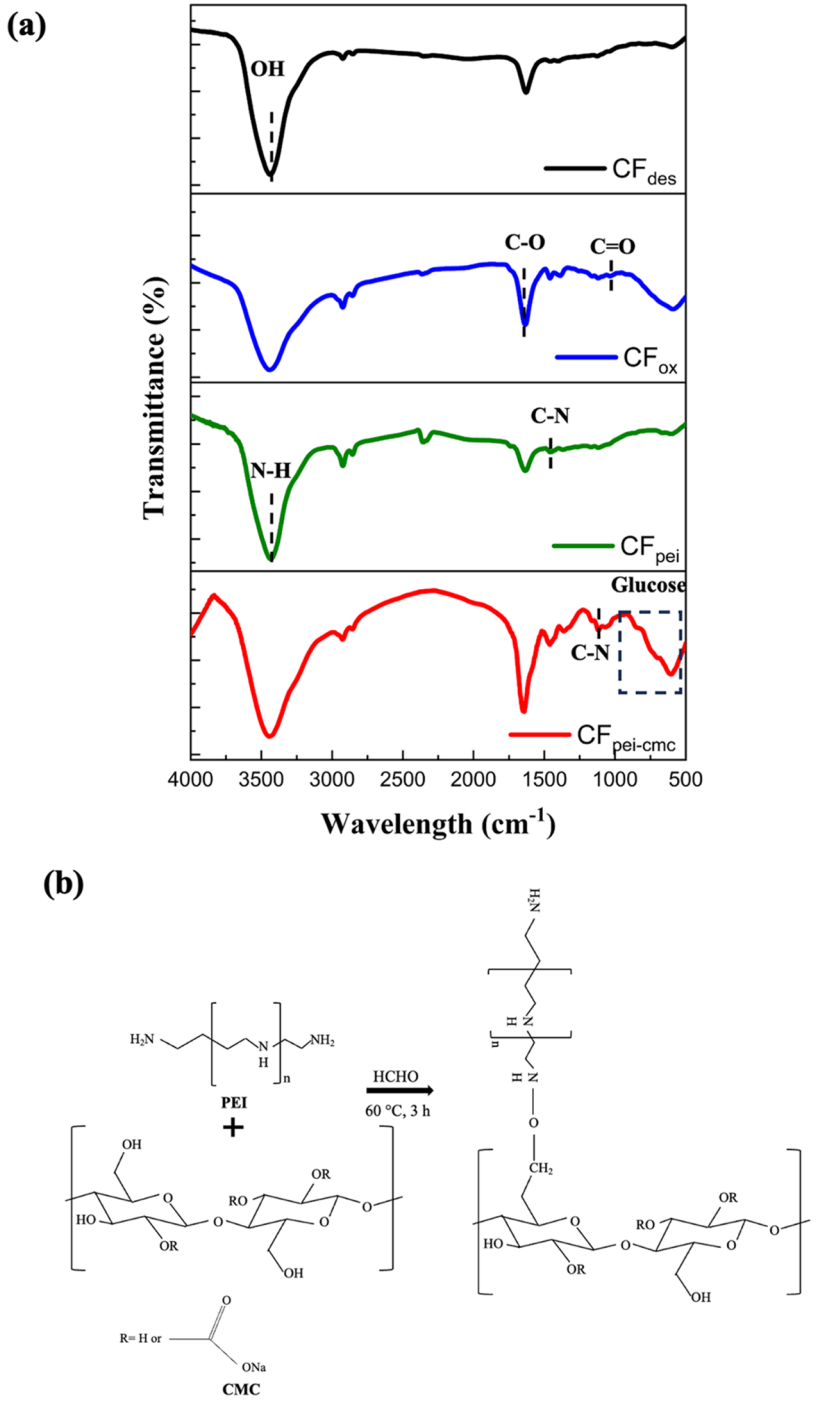

Figure 5. FTIR results of CFs (a) and the chemical reaction between PEI and CMC (b).

the peaks at approximately 284.5, 285−285.9, 286, 287−287.7, and 288.2 eV, which were attributed to C−C, C−N, C−O, N−C═O, and O−C═O, respectively.[37−40] Due to the formation of COOH groups on the surface of carbon fibers after oxidation, a more pronounced O−C═O peak was observed in the CF_{ox} sample compared to that of CF_{des}, demonstrating the significant effect of oxidation. After PEI coating, the O═C−O (288.2 eV) peak in the CF_{des} and CF_{ox} samples transformed into an N−C═O (287.7 eV) peak representing amide groups. Furthermore, a new C−N peak emerged at 287.7 eV. When PEI-CMC was grafted on the CF, N−C═O and C−N peaks were also observed. These results show that PEI and CMC can provide various functional groups and effectively adhere to the surface of CFs. Additionally, different functional groups on the surface of CFs due to PEI and CMC may enhance the interfacial bond strength.[24]

4.5. Interfacial Strength between CFs and PA6. In order to evaluate the interfacial strength between CFs and PA6, the prepared TFB sample is displayed in Figure 7(a). In relation to the TFB strength of the carbon fibers, as illustrated in Figure 7(b), a noticeable enhancement in TFB strength is evident when the carbon fibers are coated with PEI-CMC. Due to its chemical inertness, the CF exhibits the lowest TFB strength with a value of 10.8 MPa, while the formation of

https://doi.org/10.1021/acsomega.4c01284
ACS Omega 2024, 9, 32547−32556

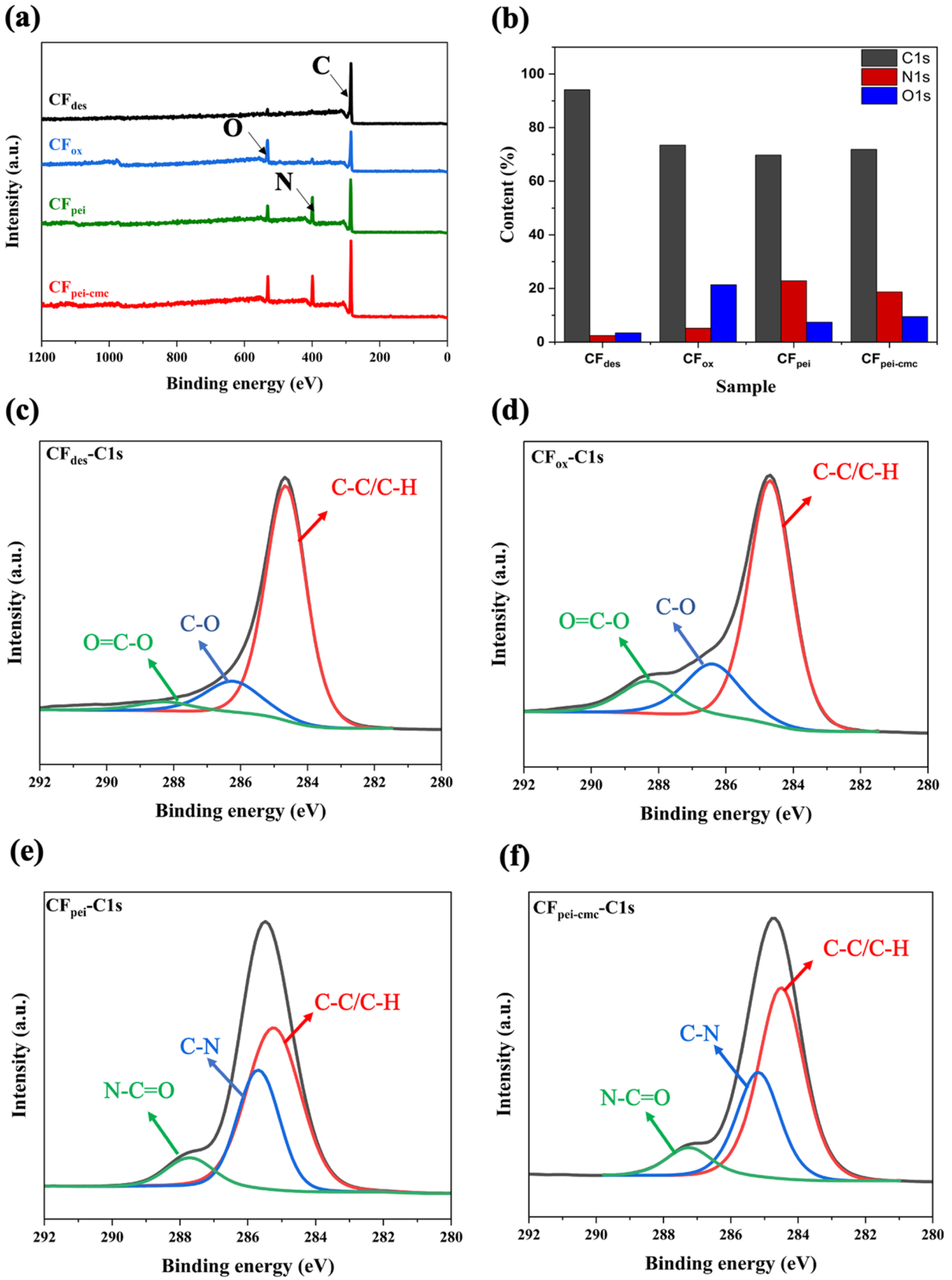

Figure 6. XPS survey spectra of different CFs (a), calculated elemental percentage (b), and high-resolution C 1s spectra of CF_{des} (c), CF_{ox} (d), CF_{pei} (e), and $CF_{pei-cmc}$ (f).

hydrogen bonds between COOH groups on the surface of the CF and PA6 after electrochemical oxidation increases the value to 12.55 MPa. The cross-linking of PEI to the CF creates hydrogen bonds between NH groups in the PEI structure and PA6, resulting in a TFB value of 21.3 MPa. The cross-linking of PEI-CMC to the CF increases the OH and NH contents in

https://doi.org/10.1021/acsomega.4c01284
ACS Omega 2024, 9, 32547−32556

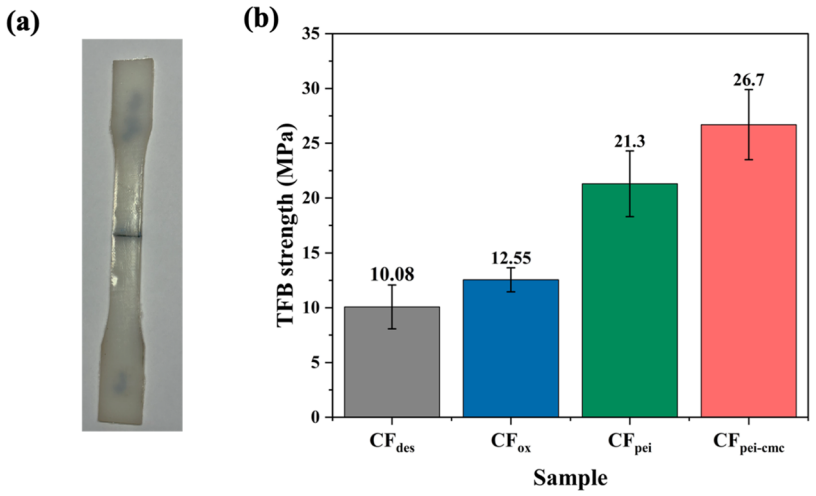

Figure 7. TFB sample (a) and TFB strength (b) of CFs.

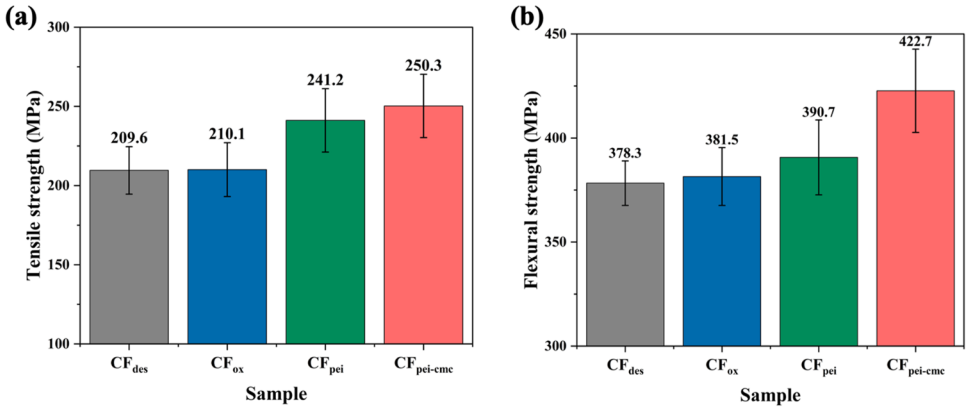

Figure 8. Tensile strength (a) and flexural strength (b) of different carbon fiber-reinforced PA6 composites.

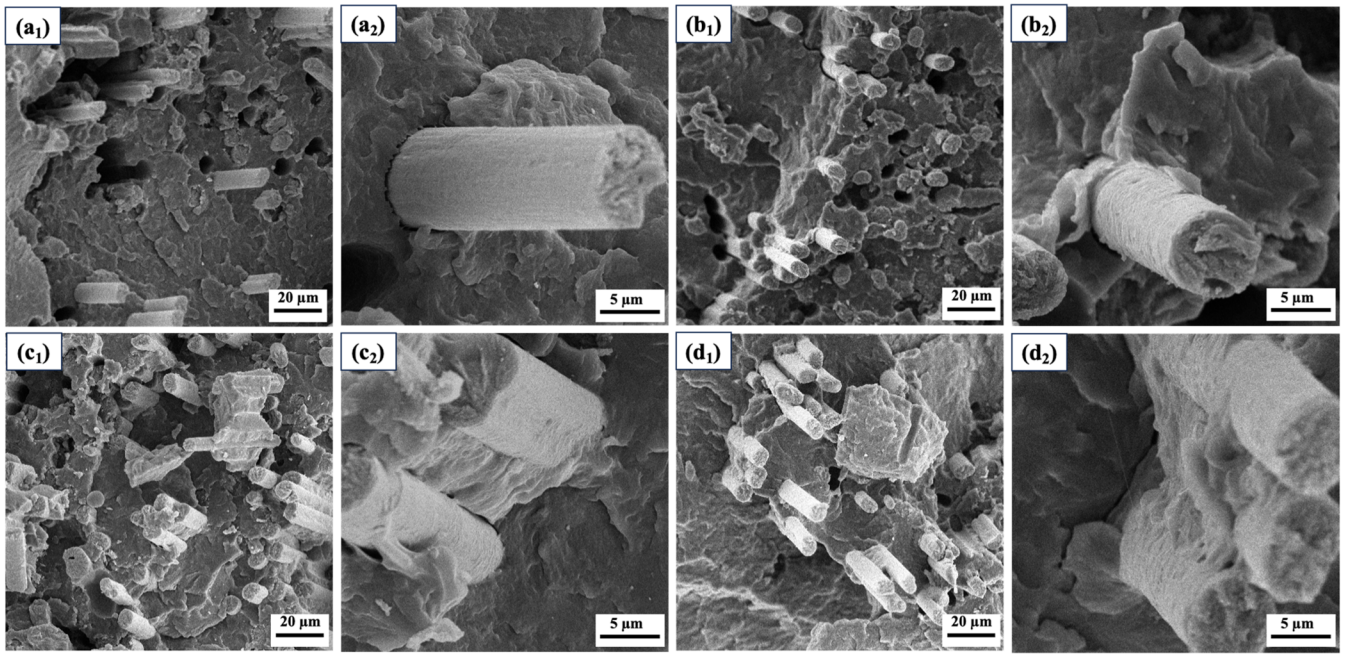

Figure 9. SEM images of the CF-reinforced PA6 fractured surface: CF_{des} (a_1, a_2), CF_{ox} (b_1, b_2), CF_{pei} (c_1, c_2), and $CF_{pei\text{-}cmc}$ (d_1, d_2).

the structure, leading to a maximum TFB strength of 26.7 MPa.

4.6. Tensile and Flexural Properties. To provide additional elucidation on the impact of the PEI-CMC sizing

https://doi.org/10.1021/acsomega.4c01284
ACS Omega 2024, 9, 32547−32556

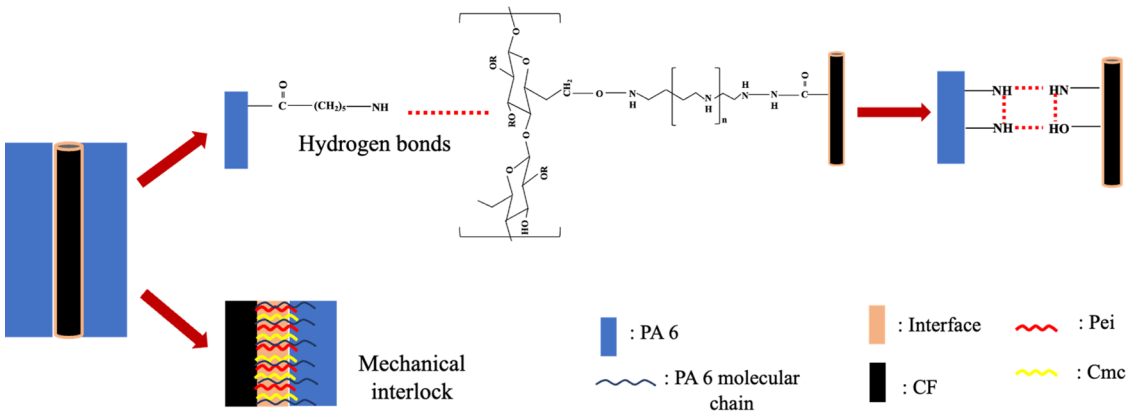

Figure 10. Schematic illustration of the interfacial bonding mechanism for the PEI-CMC-grafted CF-reinforced PA6 composite.

agent on the mechanical characteristics of CF/PA6 composites, we further assessed the tensile and flexural properties. Figure 8 displays the results of mechanical properties of carbon fiber-reinforced PA6 composites. It is clearly observed that the tensile strength of CF-reinforced PA6 composites with surface treatments had slightly increased. The tensile strengths of CF_{des}, CF_{ox}, CF_{pei}, and $CF_{pei\text{-}cmc}$ were 209.6, 210.1, 241.2, and 250.3 MPa, respectively. The high interfacial bonding facilitates the transfer of stress between reinforcement and the matrix, consequently enhancing the tensile strength of PEI-CMC-sized CF/PA6 composites. The flexural strength for $CF_{pei\text{-}cmc}$ was found to be 422.7 MPa, which was 11.7% higher than that of CF_{des}. It is widely accepted that the tensile stress and interlaminar shear stress occur concurrently during flexural loading. Hence, the enhancement in flexural properties of PEI-CMC-sized CF/PA6 composites is also acceptable.

Figure 9 shows the SEM images of the tensile fracture surface of carbon fiber-reinforced PA6 composites. The noticeable extraction of untreated CFs from the PA6 matrix, accompanied by the nearly smooth surfaces of the carbon fibers, clearly indicates a poor interfacial bonding between PA6 and untreated CF. Hence, interfacial debonding readily occurs at the interface, resulting in composite failure. After surface treatments (oxidation, PEI grafting, and PEI-CMC grafting), the pull-out fibers in CF_{ox}, CF_{pei}, and $CF_{pei\text{-}cmc}$ were reduced; however, the pull-out still continued for some fibers. The remaining PA6 polymer on the pulled-out fiber surface indicated that the interfacial bonding had slightly improved, which was supported by a 164.8% increase in the TFB value. The increase in interfacial adhesion was observed to result in an enhancement in tensile and flexural strengths.

4.7. Interfacial Bonding Mechanism. The schematic representation of the interfacial bonding mechanism of the PEI-CMC-grafted CF-reinforced PA6 composite is provided in Figure 10. Here, it is possible due to two different mechanisms: first, the formation of hydrogen bonding between the OH and NH functional groups created on the surface of carbon fibers and the NH groups of PA6. Second, mechanical interlocking due to the irregularities created on the surface by the PEI-CMC grafted onto it, which enables the polymer to infiltrate it. Under load, the PEI-CMC acts as a connector at the interface, potentially decreasing the probability of interface cracking and the pull-out of carbon fibers.

5. CONCLUSIONS

CF reinforcement was successfully prepared with water-based sizing materials obtained from grafting PEI with CMC. FTIR and XPS results of $CF_{pei\text{-}cmc}$ indicated that the grafting reaction of PEI-CMC was successfully realized. Due to the formation of functional groups, the contact angle of $CF_{pei\text{-}cmc}$ decreased to 26.42° from 111.69°. Compared with the virgin CF, the tensile strength, flexural strength, and TFB strength of $CF_{pei\text{-}cmc}$ increased by about 19.3%, 11.7%, and 164.8%, respectively. The high mechanical performances were ascribed to two perspectives: the hydrogen bonds established between amino groups of PEI-CMC and amide groups of PA6 and the mechanical interlock constructed by penetrating polymer molecules into the PEI-CMC film at the interface. Hence, the PEI-CMC-modified CFs could notably improve the mechanical characteristics of the PA6/PEI-CMC−CF composite by enhancing the interfacial properties. In addition, because of its simplicity, convenience, environmental friendly nature, and commercial availability, the method employed in this study may be applicable to other thermoplastic composites reinforced with fibers.

AUTHOR INFORMATION

Corresponding Author

Ali Kilic − *Department of Textile Engineering, Istanbul Technical University, Istanbul 34437, Turkey;* orcid.org/0000-0001-5915-8732; Email: alikilic@itu.edu.tr

Authors

Emine C. Gokce − *Department of Metallurgical and Materials Engineering, Istanbul Technical University, 34469 Istanbul, Turkey;* orcid.org/0000-0003-0792-1921

Melike Gungor − *Department of Textile Engineering, Istanbul Technical University, Istanbul 34437, Turkey*

Mahmut Ercan Acma − *Department of Metallurgical and Materials Engineering, Istanbul Technical University, 34469 Istanbul, Turkey*

Complete contact information is available at: https://pubs.acs.org/10.1021/acsomega.4c01284

Notes

The authors declare no competing financial interest.

https://doi.org/10.1021/acsomega.4c01284
ACS Omega 2024, 9, 32547−32556

■ ACKNOWLEDGMENTS

The authors gratefully acknowledge AREKA Advanced Technologies Ltd. for using their Lab Scale LFRT line during the experiments.

■ REFERENCES

(1) Stieven Montagna, L.; Ferreira de Melo Morgado, G.; Lemes, A. P.; Roberto Passador, F.; Cerqueira Rezende, M. Recycling of carbon fiber-reinforced thermoplastic and thermoset composites: A review. *J. Thermoplast Compos Mater.* **2023**, *36* (8), 3455−3480.

(2) Yan, C.; Zhu, Y.; Liu, D.; Xu, H.; Chen, G.; Chen, M.; Cai, G. Improving interfacial adhesion and mechanical properties of carbon fiber reinforced polyamide 6 composites with environment-friendly water-based sizing agent. *Composites, Part B* **2023**, *258*, No. 110675.

(3) Almushaikeh, A. M.; Alaswad, S. O.; Alsuhybani, M. S.; AlOtaibi, B. M.; Alarifi, I. M.; Alqahtani, N. B.; Aldosari, S. M.; Alsaleh, S. S.; Haidyrah, A. S.; Alolyan, A. A.; Alshammari, B. A. Manufacturing of carbon fiber reinforced thermoplastics and its recovery of carbon fiber: A review. *Polym. Test.* **2023**, *122*, No. 108029.

(4) Kim, S. W.; Park, T.; Um, M. K.; Lee, J.; Seong, D. G.; Yi, J. W. Effect of caprolactam modified phenoxy-based sizing material on reactive process of carbon fiber-reinforced thermoplastic polyamide-6. *Composites, Part A* **2020**, *139*, No. 106104.

(5) Pu, Y.; Ma, Z.; Liu, L.; Bai, Y.; Huang, Y. Improvement on strength and toughness for CFRPs by construction of novel "soft-rigid" interface layer. *Composites, Part B* **2022**, *236*, No. 109846.

(6) Yao, X.; Gao, X.; Jiang, J.; Xu, C.; Deng, C.; Wang, J. Comparison of carbon nanotubes and graphene oxide coated carbon fiber for improving the interfacial properties of carbon fiber/epoxy composites. *Composites, Part B* **2018**, *132*, 170−177.

(7) Sharma, M.; Gao, S.; Mäder, E.; Sharma, H.; Wei, L. Y.; Bijwe, J. Carbon fiber surfaces and composite interphases. *Compos. Sci. Technol.* **2014**, *102*, 35−50.

(8) Lee, H.; Ohsawa, I.; Takahashi, J. Effect of plasma surface treatment of recycled carbon fiber on carbon fiber-reinforced plastics (CFRP) interfacial properties. *Appl. Surf. Sci.* **2015**, *328*, 241−246.

(9) Baghery Borooj, M.; Mousavi Shoushtari, A.; Haji, A.; Nosratian Sabet, E. Optimization of plasma treatment variables for the improvement of carbon fibres/epoxy composite performance by response surface methodology. *Compos. Sci. Technol.* **2016**, *128*, 215−221.

(10) Andideh, M.; Esfandeh, M. Effect of surface modification of electrochemically oxidized carbon fibers by grafting hydroxyl and amine functionalized hyperbranched polyurethanes on interlaminar shear strength of epoxy composites. *Carbon* **2017**, *123*, 233−242.

(11) Fu, Y.; Li, H.; Cao, W. Enhancing the interfacial properties of high-modulus carbon fiber reinforced polymer matrix composites via electrochemical surface oxidation and grafting. *Composites, Part A* **2020**, *130*, No. 105719.

(12) Tiwari, S.; Bijwe, J.; Panier, S. Tribological studies on polyetherimide composites based on carbon fabric with optimized oxidation treatment. *Wear* **2011**, *271* (9), 2252−2260.

(13) Wu, Z.; Pittman, C. U.; Gardner, S. D. Nitric acid oxidation of carbon fibers and the effects of subsequent treatment in refluxing aqueous NaOH. *Carbon* **1995**, *33* (5), 597−605.

(14) Yuan, X.; Zhu, B.; Cai, X.; Zhao, S.; Qiao, K.; Zhang, M. Effects of particle size and distribution of the sizing agent on carbon fiber/epoxy composites interfacial adhesion. *Polym. Compos.* **2018**, *39* (S4), E2036−E2045.

(15) Downey, M. A.; Drzal, L. T. Toughening of carbon fiber-reinforced epoxy polymer composites utilizing fiber surface treatment and sizing. *Composites, Part A* **2016**, *90*, 687−698.

(16) Chen, Q.; Peng, Q.; Zhao, X.; Sun, H.; Wang, S.; Zhu, Y.; Liu, Z.; Wang, C.; He, X. Grafting carbon nanotubes densely on carbon fibers by poly(propylene imine) for interfacial enhancement of carbon fiber composites. *Carbon* **2020**, *158*, 704−710.

(17) Lee, G.; Sung, M.; Youk, J. H.; Lee, J.; Yu, W. R. Improved tensile strength of carbon nanotube-grafted carbon fiber reinforced composites. *Compos. Struct.* **2019**, *220*, 580−591.

(18) Xu, Z.; Chen, L.; Huang, Y.; Li, J.; Wu, X.; Li, X.; Jiao, Y. Wettability of carbon fibers modified by acrylic acid and interface properties of carbon fiber/epoxy. *Eur. Polym. J.* **2008**, *44* (2), 494−503.

(19) Cai, G.; Wada, M.; Ohsawa, I.; Kitaoka, S.; Takahashi, J. Tensile properties of recycled carbon fibers subjected to superheated steam treatment under various conditions. *Composites, Part A* **2020**, *133*, No. 105869.

(20) Wen, Z.; Xu, C.; Qian, X.; Zhang, Y.; Wang, X.; Song, S.; Dai, M.; Zhang, C. A two-step carbon fiber surface treatment and its effect on the interfacial properties of CF/EP composites: The electrochemical oxidation followed by grafting of silane coupling agent. *Appl. Surf. Sci.* **2019**, *486*, 546−554.

(21) Layek, R. K.; Kundu, A.; Nandi, A. K. High-Performance Nanocomposites of Sodium Carboxymethylcellulose and Graphene Oxide. *Macromol. Mater. Eng.* **2013**, *298* (11), 1166−1175.

(22) Saqib, M.; Khan, I.; Shafie, S. Application of Atangana−Baleanu fractional derivative to MHD channel flow of CMC-based-CNT's nanofluid through a porous medium. *Chaos, Solitons Fractals* **2018**, *116*, 79−85.

(23) Qiu, B.; Li, M.; Zhang, X.; Chen, Y.; Zhou, S.; Liang, M.; Zou, H. Carboxymethyl cellulose sizing repairs carbon fiber surface defects in epoxy composites. *Mater. Chem. Phys.* **2021**, *258*, No. 123677.

(24) Qiu, B.; Sun, T.; Li, M.; Chen, Y.; Zhou, S.; Liang, M.; Zou, H. High micromechanical interlocking graphene oxide/carboxymethyl cellulose composite architectures for enhancing the interface adhesion between carbon fiber and epoxy. *Composites, Part A* **2020**, *139*, No. 106092.

(25) Peng, Y.; Gardner, D. J.; Han, Y. Characterization of mechanical and morphological properties of cellulose reinforced polyamide 6 composites. *Cellulose* **2015**, *22* (5), 3199−3215.

(26) Kiziltas, E. E.; Yang, H. S.; Kiziltas, A.; Boran, S.; Ozen, E.; Gardner, D. J. Thermal Analysis of Polyamide 6 Composites Filled by Natural Fiber Blend. *BioResources* **2016**, *11* (2), 4758−4769.

(27) Kashani Rahimi, S.; Otaigbe, J. U. Polyamide 6 nanocomposites incorporating cellulose nanocrystals prepared by In situ ring-opening polymerization: Viscoelasticity, creep behavior, and melt rheological properties. *Polym. Eng. Sci.* **2016**, *56* (9), 1045−1060.

(28) Wang, C.; Okubayashi, S. Polyethyleneimine-crosslinked cellulose aerogel for combustion CO2 capture. *Carbohydr. Polym.* **2019**, *225*, No. 115248.

(29) Zong, E.; Huang, G.; Liu, X.; Lei, W.; Jiang, S.; Ma, Z.; Wang, J.; Song, P. A lignin-based nano-adsorbent for superfast and highly selective removal of phosphate. *J. Mater. Chem. A* **2018**, *6* (21), 9971−9983.

(30) Wang, Q.; Zheng, C.; Shen, Z.; Lu, Q.; He, C.; Zhang, T. C.; Liu, J. Polyethyleneimine and carbon disulfide co-modified alkaline lignin for removal of Pb2 + ions from water. *Chem. Eng. J.* **2019**, *359*, 265−274.

(31) Jiang, J.; Yao, X.; Xu, C.; Su, Y.; Zhou, L.; Deng, C. Influence of electrochemical oxidation of carbon fiber on the mechanical properties of carbon fiber/graphene oxide/epoxy composites. *Composites, Part A* **2017**, *95*, 248−256.

(32) Yang, L.; Han, P.; Gu, Z. Grafting of a novel hyperbranched polymer onto carbon fiber for interfacial enhancement of carbon fiber reinforced epoxy composites. *Mater. Des.* **2021**, *200*, No. 109456.

(33) Wu, G.; Chen, L.; Liu, L. Direct grafting of octamaleamic acid-polyhedral oligomeric silsesquioxanes onto the surface of carbon fibers and the effects on the interfacial properties and anti-hydrothermal aging behaviors of silicone resin composites. *J. Mater. Sci.* **2017**, *52* (2), 1057−1070.

(34) Fang, J.; Zhang, L.; Li, C. Polyamide 6 composite with highly improved mechanical properties by PEI-CNT grafted glass fibers through interface wetting, infiltration and crystallization. *Polymer* **2019**, *172*, 253−264.

https://doi.org/10.1021/acsomega.4c01284
ACS Omega 2024, 9, 32547−32556

(35) Dong, H.; Ding, L.; Yan, F.; Ji, H.; Ju, H. The use of polyethylenimine-grafted graphene nanoribbon for cellular delivery of locked nucleic acid modified molecular beacon for recognition of microRNA. *Biomaterials* **2011**, *32* (15), 3875−3882.
(36) Talat, M.; Singh, A. K.; Srivastava, O. N. Optimization of process variables by central composite design for the immobilization of urease enzyme on functionalized gold nanoparticles for various applications. *Bioprocess Biosyst Eng.* **2011**, *34* (6), 647−657.
(37) Yan, C.; Zhu, Y.; Liu, D.; Xu, H.; Chen, G.; Chen, M.; Cai, G. Improving interfacial adhesion and mechanical properties of carbon fiber reinforced polyamide 6 composites with environment-friendly water-based sizing agent. *Composites, Part B* **2023**, *258*, No. 110675.
(38) Peñas-Garzón, M.; Sampaio, M. J.; Wang, Y. L.; Bedia, J.; Rodriguez, J. J.; Belver, C.; Silva, C. G.; Faria, J. L. Solar photocatalytic degradation of parabens using UiO-66-NH2. *Sep. Purif. Technol.* **2022**, *286*, No. 120467.
(39) Zhang, L.; Tu, L. yu.; Liang, Y.; Chen, Q.; Li, Z. sheng.; Li, C. hai.; Wang, Z. hui.; Li, W. Coconut-based activated carbon fibers for efficient adsorption of various organic dyes. *RSC Adv.* **2018**, *8* (74), 42280−42291.
(40) Ravi, S.; Zhang, S.; Lee, Y. R.; Kang, K. K.; Kim, J. M.; Ahn, J. W.; Ahn, W. S. EDTA-functionalized KCC-1 and KIT-6 mesoporous silicas for Nd3+ ion recovery from aqueous solutions. *J. Ind. Eng. Chem.* **2018**, *67*, 210−218.

https://doi.org/10.1021/acsomega.4c01284
ACS Omega 2024, 9, 32547−32556